

Solution Spectroscopic and Chemical Properties of the Complex Hydride $[\text{FeH}_6]^{4-}$

Donald E. Linn, Jr.,*[†] and Sidney G. Gibbins[‡]

Departments of Chemistry, Indiana University-Purdue University at Fort Wayne, Fort Wayne, Indiana 46805-1499, and University of Victoria, Victoria V8W 2Y2, Canada

Received October 31, 1996[⊗]

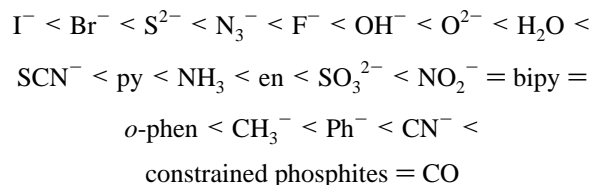
Solution spectroscopic and chemical behavior was examined in the case of the homoleptic hydridic anion of iron $[\text{FeH}_6]^{4-}$. Examination of the UV–visible spectrum in THF revealed a LMCT band which occurs at $41 \times 10^3 \text{ cm}^{-1}$ ($\epsilon = 1200 \text{ L mol}^{-1} \text{ cm}^{-1}$). A manifold between 470 and 500 nm was consistent with overlapping spin-forbidden transitions: $^1\text{A}_{1g} \rightarrow ^3\text{T}_{2g}$ and $^1\text{A}_{1g} \rightarrow ^3\text{T}_{1g}$. The doubly spin-forbidden transition ($^1\text{A}_{1g} \rightarrow ^5\text{T}_{2g}$) was not observed. Spin-allowed ligand field transitions, $^1\text{A}_{1g} \rightarrow ^1\text{T}_{2g}$ and $^1\text{A}_{1g} \rightarrow ^1\text{T}_{1g}$, occurred at 28.2 ($\epsilon = 356 \text{ L mol}^{-1} \text{ cm}^{-1}$) and $24.2 \times 10^3 \text{ cm}^{-1}$ ($\epsilon = 414 \text{ L mol}^{-1} \text{ cm}^{-1}$), respectively. The latter data yielded the parameters $\Delta_{\text{H}^-} = 25 \times 10^3 \text{ cm}^{-1}$ and $B = 310 \text{ cm}^{-1}$, assuming $C/B = 4$. Thus, the position of hydride was established in the spectrochemical series of low-spin Fe^{2+} as well beneath cyanide ($35 \times 10^3 \text{ cm}^{-1}$) yet well above bipyridine ($18 \times 10^3 \text{ cm}^{-1}$). Titration of solutions of $[\text{FeH}_6][\text{MgX}(\text{THF})_2]_4$ ($1.2 \times 10^{-3} \text{ M}$), **I** ($X = \text{Cl, Br}$), with $[\text{MgCl}_2]$ ($(1.8\text{--}45) \times 10^{-3} \text{ M}$) did not perturb the ligand field absorptions but caused a hypsochromic shift in the LMCT band consistent with the formation of the less anionic polyhydride complex, **I**, from $[\text{MgX}(\text{THF})_n]^+$ and $\{[\text{FeH}_6][\text{MgX}(\text{THF})_2]_3\}^-$, **II**, where $K_1 \approx (3 \pm 1) \times 10^{-3}$ (UV–visible). The ^1H NMR ($1.2 \times 10^{-3} \text{ M}$, 25°C) in THF- d_8 displayed two hydride components at $\delta -20.3$ and -20.4 ppm (5.6:1). Coalescence of the two hydride absorptions occurred near 40°C and 200 MHz. Reaction of **I** with $^6\text{LiOH}$ (8 equiv) was found by $^6\text{Li}\{^1\text{H}\}$ NMR to result in the replacement of the $[\text{MgX}]^+$ unit in **I** with $^6\text{Li}^+$.

Introduction

Transition metal hydride compounds in which hydrogen is the only ligand, *i.e.* the homoleptic hydrides, are interesting from several standpoints. First, the stoichiometric density of hydrogen at the metal center is extremely high for such species, as, for example, the 9:1 ratio which is seen in Ginsberg's nonahydride, $\text{K}_2[\text{ReH}_9]$.¹ Further, they represent species which are unambiguous examples of strictly transition metal hydride bonding. A number of these compounds have accumulated which can be described as either principally covalent or intermetallic complex hydrides.²

The soluble hexahydroferrate(II) $[\text{FeH}_6][\text{MgX}(\text{THF})_2]_4$, **I**, has been prepared by S.G.G. and its structure characterized by X-ray and neutron diffraction.³ These studies established the existence of octahedral $[\text{FeH}_6]^{4-}$ in which the short Fe–H bond (1.609 Å) indicated a covalent bond. Four $[\text{MgX}(\text{THF})_2]^+$ units were positioned in a tetrahedral geometry on alternate faces of the $[\text{FeH}_6]^{4-}$ octahedron. A long Mg–H bond (2.095 Å) indicated an ionic interaction. Magnetic susceptibility and Mössbauer measurements on **I** established that **I** was low-spin d^6 $[\text{Fe}(\text{II})]$.⁴ Further, the present study takes the opportunity to study the solution spectroscopic and chemical properties of an example of this less ordinary class of compounds.

The position of the hydride ligand in the spectrochemical series has remained an unresolved issue. An abbreviated order can be represented by the following sequence:⁵



Wilkinson placed the hydride ligand at about the same level as that of ammine.⁶ Bancroft used indirect Mössbauer data to position the ligand at a level higher than or about the same as that of cyanide.⁷ Further, Chatt concluded that hydride and methide occupied approximately the same position.⁸ Unlike earlier estimates, observation of the electronic absorption spectrum of **I** in THF yields information on the purely hydridic ligand field absorptions of $[\text{FeH}_6]^{4-}$. From these data, it is possible to deduce the effects of the ligand field stabilization energy parameter, Δ_{H^-} , on the octahedral environment of the ferrous ion. The position of the hydride ligand in the spectrochemical series is deduced thereby unambiguously.

Proton NMR is a sensitive probe of the environment of the hydride ligand in solution and provides a picture of the solution structure. One earlier report indicated a single line, consistent with a single octahedral complex.^{3b} Our recent data indicate that two species are present, which are related by chemical exchange.

A goal of this study is to establish the relationship between a strong-field ligand, like cyanide, which is capable of π -back-bonding, and the hydride ligand, which is capable of only

* To whom correspondence should be addressed.

[†] Indiana University-Purdue University at Fort Wayne.

[‡] University of Victoria.

[⊗] Abstract published in *Advance ACS Abstracts*, July 1, 1997.

- (1) (a) Ginsberg, A. P.; Miller, J. M.; Koubek, J. *Am. Chem. Soc.* **1961**, *83*, 4909. (b) Abrahams, S. C.; Ginsberg, A. P.; Knox, K. *Inorg. Chem.* **1964**, *3*, 558.
- (2) (a) Brönger, W. *Angew. Chem., Int. Ed. Engl.* **1991**, *30*, 759. (b) Yvon, K. Hydrides: Solid State Transition Metal Hydride Complexes. In *Encyclopedia of Inorganic Chemistry*; King, R. B., Ed.; Wiley: New York, 1994; p 1401.
- (3) (a) Gibbins, S. G. *Inorg. Chem.* **1977**, *16*, 2571. (b) Bau, R.; Chiang, M. Y.; Ho, D. M.; Gibbins, S. G.; Emge, T. J.; Koetzle, T. F. *Inorg. Chem.* **1984**, *23*, 2833. (c) The actual formulation of **I** is $[\text{FeH}_6][\text{MgX}(\text{THF})_2]_4$, where $X = \text{Cl}_{0.12}\text{Br}_{0.88}$. This does not affect the interpretation of the results that follow because halides are principally "spectator ions", and throughout this paper **I** will be referred to as simply $[\text{FeH}_6][\text{MgCl}(\text{THF})_2]_4$.

(4) Moyer, R. O., Jr.; Lindsay, R.; Suib, S.; Zerger, R. P.; Tanaka, J.; Gibbins, S. G. *Inorg. Chem.* **1985**, *24*, 3890.

(5) Lever, A. B. P. *Inorganic Electronic Spectroscopy*; Elsevier: Amsterdam, 1984; Chapter 9.

(6) Thomas, K.; Osborn, J. A.; Wilkinson, G. *J. Chem. Soc. A* **1968**, 1801.

(7) Bancroft, G. M.; Mays, M. J.; Prater, B. E. *J. Chem. Soc., Chem. Commun.* **1969**, 39.

(8) Chatt, J.; Hayter, R. G. *J. Chem. Soc. A* **1961**, 772.

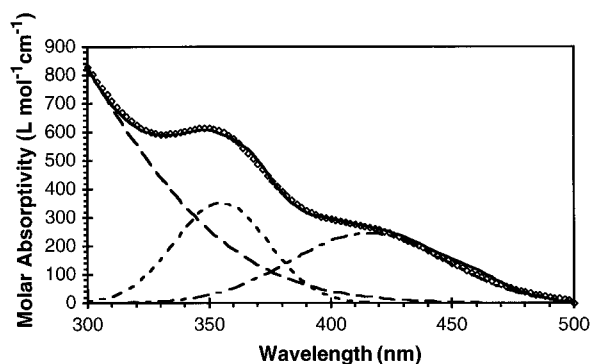


Figure 1. UV-visible spectrum of $[\text{FeH}_6][\text{MgCl}(\text{THF})_2]_4$ in THF. Conditions: concentration = 9.80×10^{-4} M; temperature = 22°C ; optical path length = 10 mm. The solid line is the observed spectrum, and the points (\diamond) are calculated to give the resolved spectrum. Parameters used to fit to the spectrum: $\lambda_1 = 250$ (15) nm; $\epsilon_1 = 1400$ (240) $\text{L mol}^{-1} \text{cm}^{-1}$; $\delta_1 = 14.5$ (2.7) $\times 10^3 \text{cm}^{-1}$; $\lambda_2 = 355$ (1) nm; $\epsilon_2 = 360$ (20) $\text{L mol}^{-1} \text{cm}^{-1}$; $\delta_2 = 4.3$ (0.2) $\times 10^3 \text{cm}^{-1}$; $\lambda_3 = 414$ (1) nm; $\epsilon_3 = 250$ (10) $\text{L mol}^{-1} \text{cm}^{-1}$; $\delta_3 = 5.3$ (0.2) $\times 10^3 \text{cm}^{-1}$ (the δ values represent bandwidths at half-height, and the numbers in parentheses are standard deviations).

σ -bonding. Further, the solution properties of the transition metal homoleptic hydrides provide relevant information on related solid state hydrides.

Experimental Section

The complex hydride $[\text{MgX}(\text{THF})_2]_4(\text{FeH}_6)$ was prepared using methods previously described in the literature and handled under inert gas (drybox) or under vacuum ($<10^{-6}$ Torr).^{3a} Magnesium chloride (99.99%), $^6\text{LiOH}\cdot\text{H}_2\text{O}$, and the adamantanol (abbreviated AdOH) were obtained from Aldrich. Both adamantanol [adamantanol-*d* (AdOD) was prepared from LiOAd and D_2O] were sublimed at 50°C under vacuum (10^{-3} Torr), and diphos (Aldrich) was recrystallized twice from hot hexane. $^6\text{LiOH}\cdot\text{H}_2\text{O}$ was dried at 150°C under vacuum (10^{-3} Torr). Solvents including pentane, THF, and THF-*d*₈, were distilled from Na/K alloy or sodium benzophenone ketyl. The THF solvents were freeze-pump-thaw-degassed three times and transferred on a high-vacuum line. The hydrogen and deuterium were of ultrahigh and research grades, respectively. Inert gases were purified by oxygen and moisture absorbers.

NMR spectra were obtained in Young valve or flame-sealed NMR tubes. IR samples were pellets (KBr) pressed or prepared as Nujol mulls and sealed between salt plates with silicone grease in the drybox. UV-visible measurements required the use of a 10 mm quartz cuvette sealed with a high-vacuum stopcock closure. All samples were prepared in a drybox or under vacuum atmosphere.

The 500 MHz ^1H NMR spectra were obtained on a Varian VXR500S, and the ^{35}Cl , ^6Li , ^2H , and ^{31}P NMR were obtained on a Varian XL200 spectrometer operating at 19.6, 29.4, 30.7, and 80.1 MHz, respectively. NMR spectra, except those of ^2H , were referenced to δ 0 ppm using aqueous solutions of 0.2 M NaCl, 3 M LiClO_4 , and 85% H_3PO_4 , respectively. FTIR were recorded on a Nicolet Magna interferometer. HP5451 and Cary 1 spectrophotometers were used to obtain the UV-visible results. The UV-visible absorption spectrum was fitted using an equation incorporating a Gaussian function which had three parameters.⁹ A linear combination of three such exponentials was refined using a standard nonlinear least-squares routine.

Results

Electronic Absorption Spectrum. Figure 1 depicts the room-temperature electronic absorption spectrum of $[\text{FeH}_6]^{4-}$ in THF. Low-temperature measurements failed due to the lack of solubility. Such measurements have not been required to

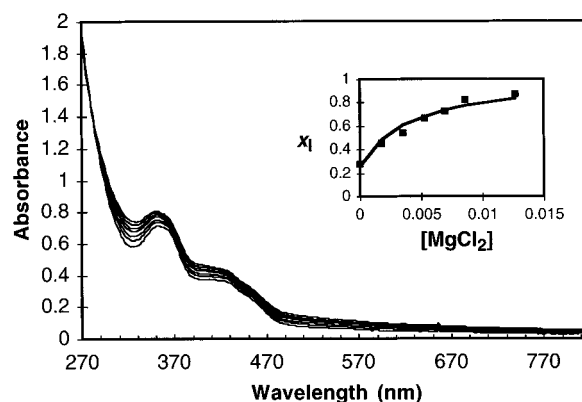


Figure 2. Titration of the UV-visible spectrum of $[\text{FeH}_6][\text{MgCl}(\text{THF})_2]_4$ in THF with $[\text{MgCl}_2]$. Conditions: concentration = 1.20×10^{-3} M; $[\text{MgCl}_2] = 0, 1.78 \times 10^{-3}, 3.53 \times 10^{-3}, 5.24 \times 10^{-3}, 6.92 \times 10^{-3}, 8.57 \times 10^{-3},$ and 12.6×10^{-3} M; temperature = 22°C ; optical path length = 10 mm. The inset shows the dependence of the mole fraction of complex I, x_1 , on $[\text{MgCl}_2]$ (see text).

deduce Δ_{H^-} , the d-orbital splitting energy of hydride, and β , the nephelauxetic parameter.

Prior to the onset of charge transfer, Figure 1 shows two major absorptions, one centered at 414 nm and another at 355 nm. There are an additional very weak absorption at *ca.* 370 nm and a broader shoulder in the range 450–470 nm.

Qualitative interpretation of this spectrum is possible by adopting the conventional methods used to describe the absorption spectra of transition metal complexes. The results of Tanabe and Sugano for the d^6 configuration show the effects of the splitting of atomic energy levels as a function of the ligand field strength.¹⁰ The diagram for low-spin d^6 $[\text{Fe}(\text{II})]$ shows five absorptions, of which two are the spin-allowed transitions, *i.e.* $^1A_{1g} \rightarrow ^1T_{1g}$ and $^1A_{1g} \rightarrow ^1T_{2g}$, which also correspond to the major absorptions in the spectrum. Assignments of the other weaker spin-forbidden transitions are hampered by their weak intensities but may account for the broad shoulder at 450–470 nm and for the small hump in the 370 nm region.

There were no medium effects observed for these ligand field transitions. Titration of **I** with $[\text{MgCl}_2]$ results in a hypsochromic shift of the charge transfer band with an isosbestic point at 280 nm while the ligand field absorptions remain unaffected (see Figure 2).

NMR Spectral Data. The 500 MHz ^1H NMR spectrum of **I** in THF-*d*₈ is shown in Figure 3A. Two hydridic components are observed for both different preparations and recrystallized samples of **I**. The major absorption ($\approx 85\%$) is centered at $\delta -20.32$ ppm ($\nu_{1/2} = 7.9$ Hz) with an adjacent peak at -20.38 ppm ($\nu_{1/2} = 9.4$ Hz). Coalescence of these peaks occurs at 40°C (200 MHz). The measured spin-lattice relaxation times are the same for the two hydride absorptions, 0.396 ± 0.002 and 0.34 ± 0.05 s (22°C and 500 MHz), respectively. The broadening is attributed to a short T_2 due to chemical exchange or the hydridic hydrogens being in the vicinity of quadrupolar nuclei (^{25}Mg).¹¹ The addition of $[\text{MgCl}_2]$ (≥ 0.015 M) results in complete conversion to a single species ($\delta -20.5$ ppm), whose line shape is dependent on temperature and $[\text{MgCl}_2]$, narrowing at higher $[\text{MgCl}_2]$ (Figure 3B) and higher temperatures. The ^{35}Cl NMR of $[\text{MgCl}_2]$ shows the presence of a low-

(10) (a) Tanabe, Y.; Sugano, S. *J. Chem. Phys.* **1954**, *9*, 753. (b) Hormann, A. C.; Shaw, C. F. *J. Chem. Educ.* **1987**, *64*, 918.

(11) We agree with one reviewer that the quadrupolar broadening of hydride by Mg (and distant Cl) is without precedent. There is the example of quadrupolar broadening of the hydride absorptions ($\nu_{1/2} \sim 6\text{--}7$ Hz) at 20°C in $[(\text{C}_5(\text{CH}_3)_5)\text{IrH}_2\text{SiMe}_3\text{Li}(\text{pmde})]$, where a ^7Li -H bond exists: Gilbert, T. M.; Bergman, R. G. *J. Am. Chem. Soc.* **1985**, *107*, 6391. ^{25}Mg (10.1%) is 9.3-fold less abundant than ^7Li (92.6%), but the magnitude of its quadrupolar moment is 6-fold that of ^7Li .

(9) (a) Henri, V.; Bielecki, J. Z. *Phys.* **1913**, *14*, 516. (b) Mead, A. *Trans. Faraday Soc.* **1934**, *30*, 1052. (c) Jørgenson, C. K. *Acta Chem. Scand.* **1955**, *8*, 1445.

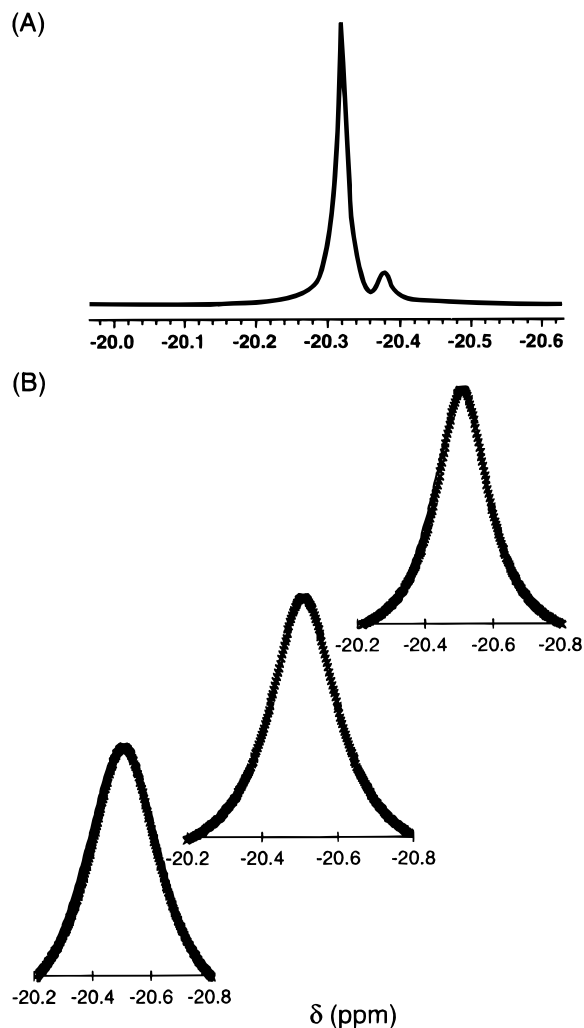


Figure 3. 500 MHz ^1H NMR spectra of (A) **I** (1.0×10^{-3} M) in $\text{THF-}d_8$ at 22 $^\circ\text{C}$ and (B) **I** (1.2×10^{-3} M) in $\text{THF-}d_8$ with the addition of 0.020, 0.12, and 0.20 M $[\text{MgCl}_2]$ at 22 $^\circ\text{C}$. In part B, measured absorptions and calculated line shapes at 200 MHz ($\nu_{1/2} = 60, 38,$ and 34 Hz, respectively) are indicated by the symbols (\times).

field absorption ($\delta 0$, $\nu_{1/2} = 1000$ Hz) which is absent in solution spectra of **I** (Figure S1, Supporting Information).

Reactions with AdOH and AdOD. Addition of 2 equiv of AdOH to **I** at -70 $^\circ\text{C}$ upon warming to room temperature gave a new signal of an unidentified hydride at $\delta -17.2$ ppm. The analogous reaction with AdOD gave no deuterides (by ^2H NMR) or observable J_{HD} splitting in the hydride region (by ^1H NMR). These reactions with alcohol rather yielded changes in the ^1H and ^2H NMR indicative of only H_2 (HD) ($\delta \sim 5$ ppm; $J_{\text{HD}} \approx 40$ Hz) elimination. **I** under D_2 (4 atm, 65 $^\circ\text{C}$), either with or without added AdOH (2 equiv), gave no indication of H/D exchange (by ^2H NMR).¹² $[\text{FeH}_2(\text{diphos})_2]$ and $[\text{FeH}_2(\text{dmpe})_2]$ are the principal products in protonation reactions by addition of 4 equiv of the corresponding ditertiary phosphine.¹³

Infrared Spectral Data. A doublet [IR (KBr): $\nu_{\text{FeH}} = 1569, 1523$ cm^{-1}] is observed in the hydride stretching region. These

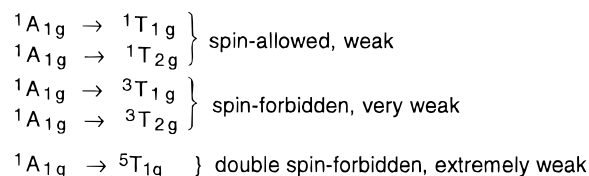
bands disappear immediately upon quenching with air. This compares with the infrared spectrum for Mg_2FeH_6 , which has symmetric stretches at $\nu_{\text{FeH}} = 1720$ cm^{-1} .¹⁴

Discussion

Determination of the Ligand Field Stabilization Parameter, Δ , and Nephelauxetic Effect, β , for the Hydride Ligand. Ginsberg has assigned the 46×10^3 cm^{-1} (217 nm; $\epsilon \sim 1800$ $\text{L mol}^{-1} \text{cm}^{-1}$) band of K_2ReH_9 in alkaline aqueous solutions to a $e'' \rightarrow a_1$ transition arising from the promotion of electron density from a σ_{H} molecular orbital predominantly on hydrogen to a σ^* molecular orbital mostly on rhenium.^{1b} The band centered at 42×10^3 cm^{-1} (250 nm; $\epsilon \sim 1400$ $\text{L mol}^{-1} \text{cm}^{-1}$) seen in Figure 1 can also be described as LMCT in origin, with the expectation that there is a shift to lower energy as the negative charge of the complex increases from -2 to -4 . Further, the blue shift for this absorption is consistent with the diminution of charge in going from a complex anion **II**, $\{[\text{FeH}_6][\text{MgCl}(\text{THF})_2]_3\}^-$, to a neutral species, **I**, $[\text{FeH}_6][\text{MgCl}(\text{THF})_2]_4$ (see Figure 2 and "Solution Chemistry of $[\text{FeH}_6]^{4-}$ ").

The qualitative approach to characterize the ligand field transitions using the classical equations of low-spin d^6 can be modified further to include effects of polarization (so-called Trees effects)¹⁵ and configurational interaction.¹⁶ The calculation of the absorption lines also includes spin-orbit coupling.¹⁹ These calculations require the wavelength maxima obtained from the resolved ligand field transitions found in Figure 1. The most uncertainty results in the determination of the charge transfer band, but this does not affect the determination of ligand field parameter, Δ_{H^-} , for the hydride ion.

The Tanabe–Sugano diagram for low-spin d^6 shows the following five low-energy Laporte-forbidden transitions:



The spin-permitted absorptions, ${}^1A_{1g} \rightarrow {}^1T_{1g}$ ($24\,200$ cm^{-1} ; $\epsilon = 414$ $\text{L mol}^{-1} \text{cm}^{-1}$) and ${}^1A_{1g} \rightarrow {}^1T_{2g}$ ($28\,100$ cm^{-1} ; $\epsilon = 356$ $\text{L mol}^{-1} \text{cm}^{-1}$), are assigned to the 414 and 355 nm absorption bands, respectively. Location of the next two weaker absorptions is hampered by a possible dynamic Jahn–Teller effect, vibrational effects, and spin-orbit coupling. Application of Schroeder's equations in the latter case indicates that each of the absorptions, ${}^1A_{1g} \rightarrow {}^3T_{1g}$ and ${}^1A_{1g} \rightarrow {}^3T_{2g}$, splits into a quartet, the lowest energy manifold of the former being nearly the same as the highest energy manifold of the latter.^{19,20} Thus, under these conditions, it is not possible to assign the spin-forbidden transitions. A likely possibility previously mentioned is that these contribute to the 450–470 nm shoulder. The ${}^1A_{1g}$

(14) Didisheim, J. J.; Zolliker, P.; Yvon, K.; Fischer, P.; Schefer, J.; Gubelmann, M.; Williams, A. F. *Inorg. Chem.* **1984**, *23*, 1953.

(15) Trees, R. E. *Phys. Rev.* **1951**, *83*, 756.

(16) Energies of configurations according to the standard equations: $\Delta E({}^1A_1 \rightarrow {}^1T_1) = \Delta - C + (86B^2/\Delta) + [8\alpha]$; $\Delta E({}^1A_1 \rightarrow {}^1T_2) = \Delta + 16B - C + (2B^2/\Delta) - [8\alpha]$; $\Delta E({}^3A_1 \rightarrow {}^3T_1) = \Delta - 3C + (50B^2/\Delta) + [8\alpha]$; $\Delta E({}^1A_1 \rightarrow {}^3T_1) = \Delta + 8B - 3C + (14B^2/\Delta) - [8\alpha]$; $\Delta E({}^1A_1 \rightarrow {}^5T_2) = 2\Delta - 5B - 8C + (120B^2/\Delta) - [8\alpha]$. Terms in parentheses are corrections from configuration interaction accounting for off-diagonal elements in the electrostatic matrices.¹⁷ Those terms in brackets represent orbit-orbit interactions or polarization corrections.¹⁸

(17) (a) Griffith, J. S. *The Theory of Transition-Metal Ions*; Cambridge University Press: London, 1961; pp 313, 412. (b) Lever, A. B. P. *Inorganic Electronic Spectroscopy*; Elsevier: Amsterdam, 1984; p 126.

(18) Here $\alpha = 67$ cm^{-1} . See ref 22b.

(19) Schroeder, K. A. *J. Chem. Phys.* **1962**, *37*, 2553.

(12) The ^2H NMR experiments with D_2 was performed in an O-ring (THF tolerant) sealed glass pressure reactor. A small amount of $\text{THF-}d_8$ (4×10^{-3} M) was added as an internal standard. AdOD (2 equiv) was added in one experiment at -70 $^\circ\text{C}$ prior to addition of D_2 . Reaction with diphos (4 equiv) at 65 $^\circ\text{C}$ overnight in THF also showed no formation of metal chelates by ^{31}P NMR.

(13) The remaining materials (25%) were characterized by ^{31}P resonances at $\delta 92$ and 81.5 ppm. Similar reactions with bis(1,2-dimethylphosphino)ethane (dmpe) gave $[\text{FeH}_2(\text{dmpe})_2]$ in even lower yield (ca. 50% by ^{31}P NMR). In the latter case the undetermined iron chelates were clearly neither $[\text{Fe}(\text{OAd})_2(\text{dmpe})_2]$ nor $[\text{FeH}(\text{OAd})(\text{dmpe})_2]$, which were prepared independently starting from $[\text{FeI}_2(\text{dmpe})_2]$.

→ ${}^5T_{2g}$ absorption would probably lie above that of ${}^1A_{1g}$ → ${}^3T_{1g}$ but would probably be very weak and thus not detectable. The slight hump at 370 nm hints at a possible location. The only unequivocal absorptions available for the determination of Δ_H are ${}^1A_{1g}$ → ${}^1T_{1g}$ and ${}^1A_{1g}$ → ${}^1T_{2g}$. This outcome is commonplace for examples of low-spin d^6 [iron(II) and cobalt(III)] complexes. The equations relating the absorptions involve Δ and the Racah parameters, B and C . Spin-forbidden transitions, which are rarely identified, make it customary to assume a C/B ratio between 4 and 5, *i.e.* comparable to that which occurs in the gas phase. For the $C/B = 4-5$ range, Δ_H varies from 24.5 to $25.0 \times 10^3 \text{ cm}^{-1}$. At an unreasonable ratio of $C/B = 9$, $\Delta_H = 25.7 \times 10^3 \text{ cm}^{-1}$.

The ligand field parameter, Δ , is a function of both the ligand and the metal ion, and accordingly placement of the ligand in a spectrochemical series is possible only when one compares various ligands on the same metal ion, in this case Fe(II). Complex **I** is the first soluble compound to be synthesized in which a transition metal is octahedrally surrounded by hydride ligands. Past efforts to deduce the position of the hydride ligand in the spectrochemical series, *i.e.* the magnitude of Δ_H , have been complicated by the presence of other ligands, *e.g.* FeHClL_4 (L = a tertiary or ditertiary phosphine ligand).⁶ Other techniques such as Jørgenson's "average" approximation have been applied; nevertheless, these methods are open to question.²¹ Hydride is generally accepted to be near cyanide (or perhaps it is even above it) in the spectrochemical series. From the spectrum of complex **I**, it is possible to conclude with certainty that hydride is high in the spectrochemical series but significantly below cyanide. This is obvious from the $\Delta E({}^1A_1 \rightarrow {}^1T_1)$ values of $31 \times 10^3 \text{ cm}^{-1}$ for $[\text{Fe}(\text{CN})_6]^{4-}$, $25.8 \times 10^3 \text{ cm}^{-1}$ for $[\text{Fe}(\text{CNO})_6]^{4-}$, and $25 \times 10^3 \text{ cm}^{-1}$ for $[\text{FeH}_6]^{4-}$.^{22,23} Clearly, hydride is higher than the group of ligands NO_2^- , bipy, and phen, the last of which has ${}^1A_1 \rightarrow {}^1T_1$ appearing at $12\,260 \text{ cm}^{-1}$.²⁴

Table 1 shows a spectrochemical series for assorted Fe(II) complexes for which polarization effects and spin-orbit coupling effects have been included for completeness. Note that H^- is below both CN^- and CNO^- but higher than diarsine and much higher than *o*-phenanthroline. Chatt's conclusion based on less direct evidence is consistent with this placement of H^- .⁸ Further, on the basis of Chatt's data, it is possible to conclude that H^- is above CH_3^- . These data contradict clearly the claims

(20) Energies of configurations using Bethe's notation: (1T_2) $\Gamma_5 = 0.984\Delta + 12.81B - 1.32C + 0.83\zeta$; (1T_2) $\Gamma_4 = 0.941\Delta + 3.05B - 1.32C + 1.29\zeta$; (3T_2) $\Gamma_2 = 0.928\Delta + 7.70B - 2.57C + 1.48\zeta$; $\Gamma_3 = 0.954\Delta + 6.32B - 2.70C + 1.26\zeta$; $\Gamma_3 = 0.947\Delta + 4.34B - 2.58C + 1.22\zeta$; $\Gamma_4 = 0.989\Delta + 1.78B - 2.35C + 0.63\zeta$; (3T_1) $\Gamma_4 = 0.959\Delta + 1.52B - 2.48C + 1.08\zeta$; $\Gamma_1 = 0.942\Delta + 0.36B - 2.70C + 1.37\zeta$; $\Gamma_5 = 0.964\Delta + 0.68B - 2.53C + 0.28\zeta$; $\Gamma_3 = 0.978\Delta + 0.95B - 2.66C + 0.61\zeta$. $\zeta = 350 \text{ cm}^{-1}$, (1T_1) = $240\,380 \text{ cm}^{-1}$, (1T_2) = $28\,170 \text{ cm}^{-1}$, and $C/B = 4$ yield the following absorptions (nm): (3T_2) 423, 423, 436, 438; (3T_1) 446, 460, 457, 467. The manifold shifts to higher wavelengths (440–490 nm) as C/B increases to 5. Negligible differences were obtained for Δ and B when these equations were solved and the results were compared to the energies obtained above (see ref 17).

(21) Jørgensen, C. K. *Absorption Spectra and Chemical Bonding in Complexes*; Pergamon: Oxford, U.K., 1962; Chapter 6.

(22) (a) Alexander, J. J.; Gray, H. B. *J. Am. Chem. Soc.* **1968**, *90*, 4260. (b) König, E.; Schlafer, H. L. *Z. Phys. Chem. (Munich)* **1962**, *34*, 355.

(23) Beck, V. W.; Feldl, K. Z. *Anorg. Allg. Chem.* **1965**, *341*, 113.

(24) Palmer, R. A.; Piper, T. S. *Inorg. Chem.* **1966**, *5*, 864.

(25) Feltham, R. D.; Silverthorn, W. *Inorg. Chem.* **1968**, *7*, 1154.

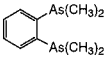
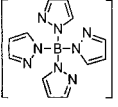
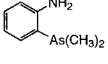
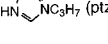
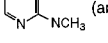
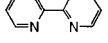
(26) Jesson, J. P.; Trofimenko, S.; Eaton, D. R. *J. Am. Chem. Soc.* **1967**, *89*, 3158.

(27) Chiswell, B.; Plowman, R. A.; Verrall, K. *Inorg. Chim. Acta* **1971**, *5*, 579.

(28) Decurtins, S.; Gütlich, P.; Hasselbach, K. M.; Hauser, A.; Spiering, H. *Inorg. Chem.* **1985**, *24*, 2174.

(29) Chum, H. L.; Vanin, J. A.; Holanda, M. I. D. *Inorg. Chem.* **1982**, *21*, 1146.

Table 1. Spectrochemical Series for Ligands Associated with Fe(II)¹

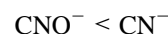
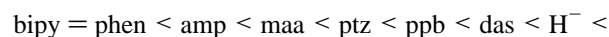
	Energy in 10^3 cm^{-1}			color of LS complex	References
	${}^1T_{1g}$	${}^1T_{2g}$	Δ		
CN^-	31	37	33	yellow	22
CNO^-	26	(32)	27.2		23
H^-	24.2	28.1	25 ²		this work
 (das)	21.4	26.6	24.5 ³	orange	25
 (ppb)	18.7	-	21 ⁴	magenta	26
 (maa)	18.3	25.4	19.5 ⁵	purple-red	27
 (ptz)	18.4	26.7	19.2	purple	28
 (amp)	17.2	-	18.6	brown	29
 (bipy)	11.5	-	16.5-19 ⁶	red	24

¹ The data of the original authors were corrected to include configuration interaction, if this correction was not applied, for the sake of comparison. Note that the first four compounds are low-spin whereas the last four are spin-crossover complexes. ² Δ_H is a lower estimate since $C/B = 4$. ³ Δ_{das} is an upper limit estimate due to the questionable assignment of 3T_1 . This calculation of Δ_{das} assumes an unlikely C/B of 10.6; a lower value for Δ_{das} is more likely. ⁴ Δ_{ppb} assumes values of $B = 800 \text{ cm}^{-1}$ and $C/B = 4.5$. ⁵ Δ_{maa} was taken from an energy level diagram; no C/B was assumed; implicitly $C/B = 4$. ⁶ This is an estimate, since charge transfer which begins at $15 \times 10^3 \text{ cm}^{-1}$ obscures 1T_1 and 1T_2 bands.

Table 2. Nephelauxetic Effect for Assorted Ligands Associated with Fe(II)

	1T_1 (10^3 cm^{-1})	1T_2 (10^3 cm^{-1})	B (cm^{-1})	β
H^-	24.2	28.1	310	0.29
das	21.4	26.6	354	0.33
CN^-	31	37	401	0.38
CNO^-	25.9	32	414	0.39
maa	18.3	25.4	515	0.49
ptz	18.4	26.7	611	0.58

that the position of H^- must be the same as or higher than that of CN^- or that Δ for H^- is comparable to that for NH_3 . Reference to Table 1 shows that, for Fe(II), the position of H^- follows on the basis of 1T_1 and 1T_2 .



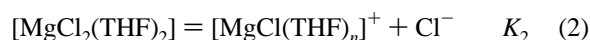
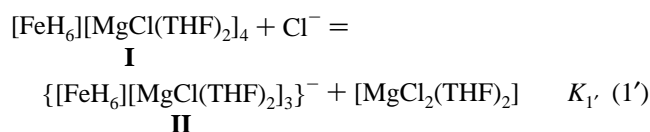
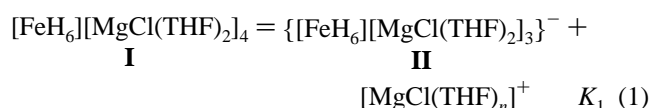
Gupta and co-workers recently performed *ab initio* density of states calculations for $\text{Mg}_2[\text{MH}_6]$ ($M = \text{Fe, Ru, Os}$), where the Δ_H are 15×10^3 , 28×10^3 , and $33 \times 10^3 \text{ cm}^{-1}$, respectively.³⁰

The nephelauxetic effect, β , is determined from the Racah B parameter, *i.e.* $\beta = B_{\text{complex}}/B_0$, which is the ratio of the interelectronic repulsion parameter for the complex to that for the free ion [$B_0 = 1058 \text{ cm}^{-1}$ for $\text{Fe}^{2+}(\text{g})$]. These values are given in Table 2 for various ligands complexed to Fe(II). The β parameter measures the ability of a ligand to promote spatial extension of the metal atom's orbitals, thereby reducing electron-electron repulsion. From Table 2, this tendency is found to be greater for hydride than for any other ligand complexed to Fe(II). This in turn supports the conclusion that

(30) Orgaz, Emilio; Gupta, Michele. *Z. Phys. Chem. (Munich)* **1991**, *181*, 1.

$[\text{FeH}_6]^{4-}$ is covalent, which is consistent with its reducing properties and the large polarizability and low electronegativity of hydrogen.

Solution Chemistry of $[\text{FeH}_6]^{4-}$. A peculiar reaction of **I** in solution is characterized by the observed changes in the ^1H NMR (Figure 2) and UV–visible spectrum upon titration with $[\text{MgCl}_2]$ (Figure 3). There are two conceivable chemical reaction pathways: the reversible loss of dihydrogen or an ion-pair reaction. The former would be difficult because of the high thermal stabilities of transition metal hydride complexes such as Mg_2FeH_6 , where decomposition occurs only above 180°C .¹⁴ Incorporation of deuterium ($p_{\text{D}_2} \approx 4$ atm) was not observable at 60°C for 12 h by ^2H NMR, nor was phosphine incorporation found by ^{31}P NMR.¹² Also absent was a peak for free molecular hydrogen. The lack of the hydrogen loss tends to rule out the inner-sphere hydrides as reaction participants. Another mode of reaction involves the addition of the Lewis acidic $[\text{MgCl}(\text{THF})_2]^+$ units onto the triangular faces of the $[\text{FeH}_6]^{4-}$ octahedron. Our data suggest an equilibrium involving the separation of $[\text{MgCl}(\text{THF})_n]^+$ from the complex ion pair, **I**, to form either a separated or solvent-separated complex ion, **II**.



Figures 2 and 3B illustrate that the addition of $[\text{MgCl}_2]$ to a solution of **I** causes the conversion into a single species assigned as **I**.³¹ Added support for this mechanism is found in the ^{35}Cl NMR spectra of solutions of **I** and MgCl_2 in THF (Figure S1, Supporting Information). MgCl_2 in THF has a prominent signal in the high-field region ($\delta 0 \pm 50$ ppm; $\nu_{1/2} = 1000$ Hz), indicative of the chloride dissociation of reaction 2.³²

The facile dissociation of the $[\text{MgCl}(\text{THF})_n]^+$ complex ion from **I** should permit the incorporation of other metal cations. This has been accomplished in the reaction of $^6\text{LiOH}$ with **I**.³³ The $\{^1\text{H}\}^6\text{Li}$ NMR of ^6Li -exchanged **I** upon broad-band irradiation gives an NOE based on integrations of 1.4 (or 41% of the theoretical maximum) (Figure S2, Supporting Information).³⁴ Further, these enhancements were recorded only when

(31) The titration of a solution of **I** with $[\text{MgCl}_2]$ yields an equilibrium quotient for the chemical exchange, $K_1 = K_1'K_2 \approx (3 \pm 1) \times 10^{-3}$ (22°C). The mole fraction of species **I**, x_1 , is given by the following relationship assuming $[\text{I}]_{\text{tot}} = [\text{I}] + [\text{II}]$, $[\text{MgCl}(\text{THF})_n]^+ \approx [\text{MgCl}_2]_{\text{tot}}$, and $[\text{II}] = \Delta A_{340}/\Delta \epsilon_{340}$ (see Figure 2):

$$x_1 = 1 - \{([\text{MgCl}_2]_{\text{tot}} + K_1) + \sqrt{([\text{MgCl}_2]_{\text{tot}} + K_1)^2 + 4[\text{I}]_{\text{tot}}K_1}\} (2[\text{I}]_{\text{tot}})^{-1}$$

(32) Akitt, J. W. In *Multinuclear NMR*; Mason, J., Ed.; Plenum: New York, 1987; Chapter 17.

(33) The metathetical replacement reaction was performed by stirring a solution of 51 mg (0.050 mmol) **I** in 10 mL of THF with 10 mg (0.40 mmol) of $^6\text{LiOH}$ overnight at 65°C . Filtration and evaporation of the solvent yield 25 mg of the tannish yellow ^6Li derivative of **I**. Data for ^6Li -**I**: ^1H NMR (THF- d_8 , 22°C , 200 MHz) $\delta -20.4$ ppm (br s); $^6\text{Li}\{^1\text{H}\}$ NMR (THF- d_8 , 22°C , 29.6 MHz) $\delta 1.1$ ppm (br s).

there was selective irradiation of the hydridic hydrogens as opposed to those of THF, which demonstrates clearly the presence of $^6\text{Li}^+$ in the outer sphere of $[\text{FeH}_6]^{4-}$ (Table S1, Supporting Information). More detailed work is necessary to disentangle the potential pathways for reaction on the surface of $[\text{FeH}_6]^{4-}$.³⁵

Conclusions

The position of the hydride ligand in the spectrochemical series has been established. Hydride is somewhat below cyanide and cyanate but above diarsine. Even though hydride has no π -back-bonding properties, it is capable of exerting a strong ligand field rivaling the best of metal complexing agents. The ability of hydride to exert its strong d-orbital splitting in the absence of π -acceptor strength points out the importance of its polarizability. For example, the cyanide complexes $[\text{M}(\text{CN})_6]^{4-}$ ($\text{M} = \text{Fe}, \text{Ru}, \text{Os}$) show a clear trend with ν_{CN} increasing as $\text{Os} > \text{Ru} > \text{Fe}$. This reflects the increased back-bonding for the heavier transition metals. Infrared data show the same trend for $[\text{MH}_6]^{4-}$ and also the sensitivity of ν_{MH} to the cubic cell constant a in $\text{M}^{\text{II}}\text{MH}_6$ ($\text{M} = \text{Ru}, \text{Os}$).³⁶ For $[\text{FeH}_6]^{4-}$, this sensitivity to a is also borne out with a 10% increase in a resulting in a 10% decrease in ν_{FeH} .³⁷ Clearly, spatial relationships in the complex hydrides, *i.e.* the type of cation in the lattice, and indeed in solution, can have a dramatic influence on the energetics and corresponding chemical properties of the transition metal-to-hydrogen bond.

Ion-pair reactions characterize these materials in THF. The fact that the $[\text{MgCl}(\text{THF})_2]^+$ unit is dissociable points to the predominantly ionic bonding between this cation and the hydridic anion. It remains to be seen how sensitive such reactions are to the nature of the transition metal hydride complex.

Acknowledgment. This paper is based on work supported by the U.S. Army Research Office under Grant DAAH04-94-0312. We also thank the donors of the Petroleum Research Fund, administered by the American Chemical Society, for partial support of this research. A study leave grant (for S.G.G.) from the University of Victoria and the hospitality of M. L. H. Green (Oxford University) are gratefully acknowledged. Further, we wish to acknowledge the technical skills of undergraduates Aaron Trout and Ann Wilkinson. Perry Pellechia, Purdue University, West Lafayette, IN, graciously provided the 500 MHz NMR spectra.

Supporting Information Available: ^{35}Cl and $^6\text{Li}\{^1\text{H}\}$ NMR spectra (Figures S1 and S2) and a table of NOEs (Table S1) (3 pages). Ordering information is given on any current masthead page.

IC961300D

(34) The $^6\text{Li}\{^1\text{H}\}$ NOE technique was applied previously for determining the structures of organolithium hydrides in solution: Avent, A. G.; Eaborn, C.; El-Kheli, M. N. A.; Molla, E. M.; Smith, D. J.; Sullivan, A. C. *J. Am. Chem. Soc.* **1986**, *108*, 3854.

(35) One reviewer suggested that $[\text{MgCl}(\text{THF})_n]^+$ (contained in **I**) and $[\text{MgCl}_2]$ add possibly to the unoccupied triangular faces of $[\text{FeH}_6]^{4-}$ to form $\{[\text{FeH}_6][\text{MgCl}(\text{THF})_2]_3\}^+$, **III**. Still another analogous redistribution reaction that the reviewer suggests is the formation of $\{[\text{FeH}_6][\text{Mg}_3\text{Cl}_3(\text{THF})_n]\}^+$, **III'**, from $[\text{MgCl}(\text{THF})_n]^+$ (contained in **I**) and $[\text{MgCl}_2]$. These equilibria require at least three hydride components: **I**, **II**, and **III** (or **III'**). The ^1H NMR and UV–vis titration data indicate that only two hydride components are present. Formation of **III** or an analog is more complicated and more demanding (sterically) than equilibria 1 and 2. **III** (or **III'**) cannot be ruled out entirely, however.

(36) Kritikos, M.; Noréus, D. *J. Solid State Chem.* **1991**, *93*, 256.

(37) A cubic cell constant for **I** is calculated to be 7.2 \AA as compared to 6.4 \AA for Mg_2FeH_6 .